Signal Detection in Sparse Multipath Channels

Matt Malloy and Akbar Sayeed
Electrical and Computer Engineering
University of Wisconsin, Madison, Wisconsin 53706
mmalloy@wisc.edu and akbar@engr.wisc.edu

***Abstract*—In this paper, we revisit the problem of signal detection in multipath environments. Existing results implicitly assume a rich multipath environment. Our work is motivated by physical arguments and recent experimental results that suggest physical channels encountered in practice exhibit a sparse structure, especially at high signal space dimension (i.e., large time-bandwidth product). We first present a model for sparse channels that quantifies the independent degrees of freedom (DoF) in the channel as a function of the physical propagation environment and signal space dimension. The number of DoF represents the delay-Doppler diversity afforded by the channel and, thus, critically impacts detection performance. Our focus is on two types of non-coherent detectors: the energy detector (ED) and the optimal non-coherent detector (ONCD) that assumes full knowledge of channel statistics. Results show, for a uniform distribution of paths in delay and Doppler, the channel exhibits a rich structure at low signal space dimension and then gets progressively sparser as this dimension is increased. Consequently, the performance of the detectors is identical in the rich regime. As the signal space dimension is increased and the channel becomes sparser, the ED suffers significant degradation in performance relative to the ONCD. Finally, our results show the existence of an optimal signal space dimension - one that yields the best detection performance - as a function of the physical channel characteristics and the operating signal to noise ratio (SNR).**

I. Introduction

In this paper, we revisit the well-studied problem of signal detection in a multipath fading environment [1]. Wireless multipath channels can be generally modeled as randomly time-varying linear systems. Virtually all existing works implicitly assume a *rich multipath* environment, influenced by the seminal work of Bello [2] in which he proposed the well-known wide-sense stationary uncorrelated scattering (WSSUS) model for randomly time-varying linear channels. A key motivation for revisiting the detection problem is that physical arguments as well as recent experimental results indicate that the assumption of rich multipath may be violated in physical channels encountered in practice; see, for example [3]–[6] and references therein. In particular, such channels exhibit a *sparse* structure, especially at high signal space dimension (i.e., large time-bandwidth product). For example, sparsity of multipath is the motivation for the so-called "finger-management" in RAKE receivers in spread-spectrum CDMA systems – some of the RAKE "fingers" corresponding to resolvable delays exhibit weak signal strength [7]. This effect gets even more pronounced in ultra-wideband channels in which the channel impulse response exhibits a sparse structure as well as "specular" rather than Gaussian fading [8]. Our focus is on *non-coherent* detection in sparse multipath channels. In particular, the choice of signaling duration, T, and bandwidth, W, can have a significant impact on detection performance.

Signal detection over multipath channels is an important problem in a number of applications. One motivating application is the so called *interweave* paradigm in cognitive radio. In this scenario unlicensed or secondary users opportunistically use the spectrum when the primary, or licensed, users are not communicating [9]–[11]. It is critical for secondary users to rapidly and reliably detect the presence of a primary transmitter in order to minimize harmful interference [12]. Imagine that to facilitate this detection, primary transmitters send a "beacon" signal in their licensed band, prior to data transmission. A key question is: Given a physical multipath channel between the primary transmitter and a secondary receiver, is there an optimal "beacon" signal that yields the best detection performance at the secondary receiver? We address this question in terms of the optimal signaling bandwidth W and duration T as a function of the signal-to-noise ratio (SNR) and multipath channel characteristics. Other applications include detection problems in sensor networks in which the sensors communicate their measurement data to a fusion center in a multipath environment. There is also renewed interest in radar operation over multipath environments.[1]

Figure 1 illustrates the impact of the time-bandwidth product, $N = TW$, on channel sparsity in a doubly selective multipath environment consisting of $N_p = 50$ propagation paths. The paths have equal power random gains; the path delays and Doppler shifts are randomly distributed over a delay spread of $\tau_{max} = 10\mu$s and a Doppler spread of $\nu_{max} = 200$Hz. The left panels show the time-varying frequency response and the right panels show the corresponding virtual channel representation at a sampling resolution of $\{\Delta\tau, \Delta\nu\} = \{1/W, 1/T\}$. The bandwidth W and signaling duration T increase from top to bottom. The maximum number of virtual channel coefficients is $D \approx TW\tau_{max}\nu_{max}$ and, thus, increases linearly with both T and W. At minimum signal space dimension, $\{T_{min}, W_{min}\}$, the virtual channel coefficients exhibit a *rich* structure – all channel coefficients (corresponding to resolvable delays - see Sec. II) contribute

This research was partly supported by the NSF under grant CNS 0627589

[1]For example, DARPA's multipath exploitation radar (MER) program is explicitly aimed at exploiting multipath reflections for target detection and localization in urban environments.

significant power. At a medium time-bandwidth product, $\{T_{med}, W_{med}\}$, the maximum number of virtual channel coefficients, D, is larger - but, some coefficients are nearly zero. Channel sparsity, indicated by the number of nearly vanishing virtual channel coefficients, is most pronounced at $\{T_{max}, W_{max}\}$. As we elaborate later, the number of dominant non-vanishing coefficients in the virtual channel represent the number of *statistically independent degrees of freedom (DoF)*. The number of DoF also quantifies the delay-Doppler diversity afforded by the multipath channel to combat fading and, thus, directly impacts the detection performance [1]. In particular, for a given multipath environment, there is a signaling dimension (time-bandwidth product) that minimizes the probability of missed detection (the probability of causing harmful interference in the cognitive radio set-up). The optimum signaling dimension depends on the operating SNR as well as the multipath channel characteristics.

We study the performance of two types of non-coherent detectors that require minimal knowledge about the channel: i) the energy detector (ED) that only requires knowledge of the channel delay and Doppler spreads, and ii) the optimal non-coherent detector (ONCD) that requires full knowledge of channel statistics. We assess the performance of the two detectors in terms of the error probabilities: the probability of false alarm, P_{FA}, and the probability of missed detection, P_{MD}. The performance of both detectors is characterized by the *hypo-exponential* distribution. Our results show that the performance of the two detectors is identical in rich multipath. As the multipath environment becomes sparser, the ED suffers significant loss in performance compared to the ONCD. We also study the relationship between the optimal signaling parameters (T and W) as a function of channel characteristics and the operating SNR.

The rest of the paper is organized is as follows. In Sec. II we develop the system model, in particular a model for sparse multipath channels in the general setting of doubly selective channels. Sec. III develops the detection framework and describes the ED and the ONCD. In Sec. IV we present and discuss results on the performance of the two detectors.

II. System Model

In this section, we develop the system model that serves as the basis for assessing signal detection performance. In particular, we use a sampled representation of physical multipath channels [2], [3], [13], [14] that captures the phenomenon of channel sparsity as a function of signaling parameters. We develop our model in the general context of doubly-selective channels.

A. Physical Discrete-Path Model for Multipath Channels

We begin our discussion with the *physical discrete-path model* [1] in which the (noise-free) received signal, $r(t)$, is modeled as a sum of scaled, delayed and Doppler-shifted versions of the transmit signal, $x(t)$:

$$r(t) = \sum_{n=1}^{N_p} \beta_n x(t-\tau_n) e^{j2\pi\nu_n t} \tag{1}$$

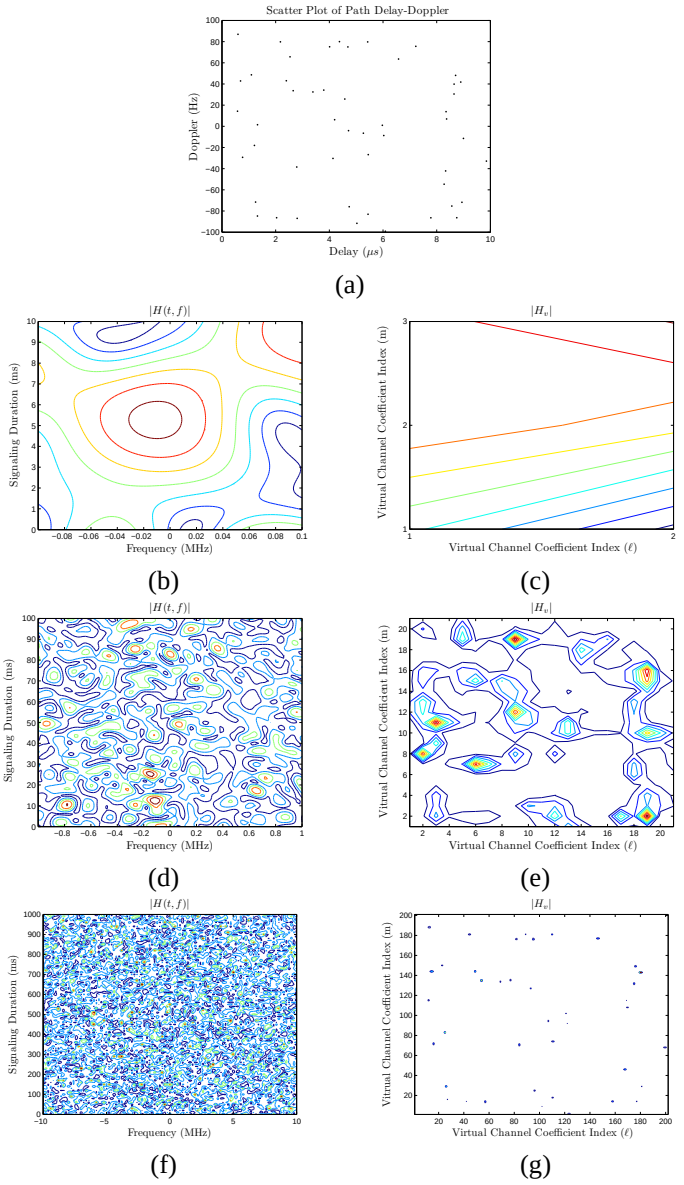

Fig. 1. Illustration of a given physical scattering environment with N_p=50, τ_{max}=10μs, and ν_{max}=200Hz when probed at different bandwidths and signaling durations. (a) shows a scatter plot of physical path delay and Doppler. Figures (b) - (g) show the magnitude of the time-varying channel frequency response $|H(t,f)|$ and the magnitude of the corresponding sampled virtual channel representation $|H_v(\ell,m)|$. (b) and (c): W_{min}=200kHz, T_{min}=10ms. (d) and (e): W_{med}=2MHz, T_{med}=100ms. (f) and (g): W_{max}=20MHz, T_{max}=1s. At high signal space dimension, all physical paths are resolvable, and (g) closely represents (a).

where $\beta_n = \alpha_n e^{j\phi_n}$ is the complex path gain, N_p is the number of discrete propagation paths, and τ_n and ν_n are the delay and Doppler shifts of the n-th path, respectively. The corresponding time-varying channel impulse response is

$$h(t,\tau) = \sum_{n=1}^{N_p} \beta_n \delta(\tau-\tau_n) e^{j2\pi\nu_n t} \tag{2}$$

where $\tau_n \in [0, \tau_{max}]$, $\nu_n \in [-\nu_{max}/2, \nu_{max}/2]$ and τ_{max} and ν_{max} are the delay and Doppler spreads of the channel [1].

The physical channel can be equivalently represented by its time-varying frequency response

$$H(t,f) \;=\; \int h(t,\tau)e^{-j2\pi f\tau}d\tau = \sum_{n=1}^{N_p}\beta_n e^{-j2\pi\tau_n f}e^{j2\pi\nu_n t}. \tag{3}$$

We assume that over the time-scales of interest, the propagation parameters $\{\beta_n,\tau_n,\nu_n\}$ remain constant. The only source of randomness are the path gains and temporal channel variations captured by the path Doppler shifts.

B. Sampled Virtual Channel Representation

For a given multipath propagation environment, as captured by the physical model, the performance of signal detection critically depends on two key signaling characteristics - the signal duration T and the (two-sided) essential signal bandwidth W - and their product, the signal space dimension, or time-bandwidth product $N = TW$. In order to quantify the interaction between the signal and the physical channel, we use a sampled virtual representation of the physical channel model that samples the delay-Doppler space at the resolution commensurate with signaling duration and bandwidth [2], [3], [14]: $\Delta\tau = 1/W$ and $\Delta\nu = 1/T$. The sampled channel representation can be construed as a truncated Fourier series representation of $H(t,f)$ induced by the restriction of $H(t,f)$ to $(t,f) \in [0,T]\times[-W/2,W/2]$ and the finite delay and Doppler spreads:

$$H(t,f) = \sum_{\ell=0}^{L-1}\sum_{m=-(M-1)}^{M-1} H_v(\ell,m)e^{j2\pi\frac{m}{T}t}e^{-j2\pi\frac{\ell}{W}f}. \tag{4}$$

The sampled virtual channel (Fourier series) coefficients can be computed as

$$H_v(\ell,m) = \frac{1}{TW}\int_0^T\int_{-W/2}^{W/2} H(t,f)e^{-j2\pi\frac{m}{T}t}e^{j2\pi\frac{\ell}{W}f}dtdf. \tag{5}$$

The limits in the series in (4) correspond to the number of resolvable delays and Doppler shifts within the channel spreads:

$$\begin{aligned} L &= \left\lceil\frac{\tau_{max}}{\Delta\tau}\right\rceil + 1 = \lceil W\tau_{max}\rceil + 1 \\ M &= \left\lceil\frac{\nu_{max}/2}{\Delta\nu}\right\rceil + 1 = \lceil T\nu_{max}/2\rceil + 1\ . \end{aligned} \tag{6}$$

The sampled virtual channel representation is illustrated in Fig. 2. It is completely characterized by the virtual channel coefficients $\{H_v(\ell,m)\}$, L and M. By substituting (3) into (5), the virtual channel coefficients can be related to the physical model as

$$\begin{aligned} &H_v(\ell,m) = \\ &\sum_{n=1}^{N_p}\beta_n e^{-j\pi(m-\nu_n T)}\mathrm{sinc}(m-\nu_n T)\mathrm{sinc}(\ell-\tau_n W) \\ &\approx \sum_{n\in S_{\tau,\ell}\cap S_{\nu,m}}\beta_n \end{aligned} \tag{7}$$

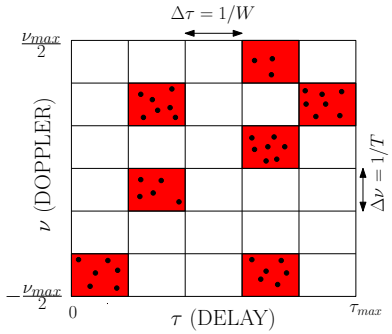

Fig. 2. Illustration of the virtual channel representation and path partitioning in delay-Doppler. Each square represents a delay-Doppler resolution bin of size $\Delta\tau\times\Delta\nu$, representing a virtual channel coefficient $H_v(\ell,m)$. Each shaded square represents a dominant non-zero coefficient with the dots representing the paths contributing to it.

where the approximation (a phase factor has been absorbed into the β_n's) is due to a key property of the virtual channel representation – *virtual path partitioning* [3], [14] as illustrated in Fig. 2: *distinct* $H_v(\ell,m)$'s correspond to (approximately) *disjoint* subsets of propagation paths. In (7), $S_{\tau,\ell}\cap S_{\nu,m}$ is the set of all paths whose delays and Doppler shifts fall within a *delay-Doppler resolution bin* of size $\Delta\tau\times\Delta\nu$ centered on the ℓ-th virtual delay (ℓ/W) and m-th virtual Doppler shift (m/T):

$$\begin{aligned} S_{\tau,\ell} &= \left\{n : \left|\tau_n - \frac{\ell}{W}\right| < \frac{1}{2W}\right\} \\ S_{\nu,m} &= \left\{n : \left|\nu_n - \frac{m}{T}\right| < \frac{1}{2T}\right\}\ . \end{aligned} \tag{8}$$

With the above sampled virtual channel representation, the physical model for the received signal (1) can be accurately approximately as

$$\begin{aligned} r(t) &= \int H(t,f)X(f)e^{j2\pi ft}df \\ &\approx \sum_{\ell=0}^{L-1}\sum_{m=-(M-1)}^{M-1} H_v(\ell,m)x\left(t-\frac{\ell}{W}\right)e^{j2\pi\frac{m}{T}t}. \end{aligned} \tag{9}$$

C. Channel Statistics, Degrees of Freedom, and Sparsity

Due to the randomness in the complex path gains, the virtual channel coefficients, $\{H_v(\ell,m)\}$, are random variables. By virtue of path partitioning, the virtual channel coefficients are *approximately* statistically independent[2]; we assume them to be exactly independent for simplicity of exposition. We also assume a Rayleigh fading scenario in which each $H_v(\ell,m)$ is a zero-mean complex Gaussian random variable. In general, this will be true when there are no line-of-sight propagation paths and if there are sufficiently many *unresolvable paths* contributing to each non-zero $H_v(\ell,m)$ so that the central limit theorem (CLT) can be invoked (see (7)). However, in

[2]The approximation gets more accurate at large T and W and for smaller values of N_p.

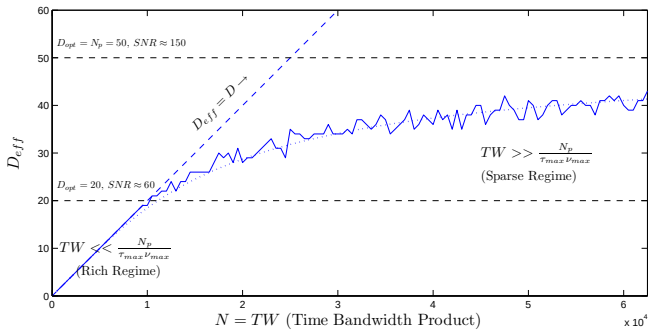

Fig. 3. Scaling of D_{eff} with N for two multipath environments with $\tau_{max} = 10\mu$s, $\nu_{max} = 200$Hz : i) idealized rich environment ($N_p = \infty$ - dashed curve), ii) physical multipath channel with $N_p = 50$ (solid curve), and iii) $E[D_{eff}]$, as defined by (15) (dotted curve). In the idealized rich channel, $D_{eff} = D = TW\tau_{max}\nu_{max}$ and scales linearly with N. However, for the physical channel with $N_p = 50$, D_{eff} initially increases linearly with N, then exhibits a sub-linear growth and eventually saturates to N_p.

this paper, we consider scenarios in which N_p is a fixed finite number. In this case, for sufficiently large bandwidths, there may be only a single physical path contributing to any non-zero $H_v(\ell)$ thereby violating the CLT.[3] Nevertheless, for simplicity, we assume Gaussian statistics for the virtual channel coefficients, which would be true if the physical path gains are modeled as zero-mean Gaussian random variables. Thus, throughout this paper $\{H_v(\ell,m)\}$ are assumed to be independent zero-mean complex Gaussian random variables:

$$\begin{aligned} H_v(\ell,m) &\sim \mathcal{CN}(0,\sigma^2_{\ell,m}) \\ \sigma^2_{\ell,m} &= E[|H_v(\ell,m)|^2] \\ &= \sum_n E[|\beta_n|^2]\mathrm{sinc}^2(\ell-\tau_n W)\mathrm{sinc}^2(m-\nu_n T) \\ &\approx \sum_{n\in S_{\tau,\ell}\cap S_{\nu,m}} E[|\beta_n|^2]\ . \end{aligned} \tag{10}$$

Note that $\{\sigma^2_{\ell,m}\}$ correspond to samples of the delay-Doppler power spectrum (scattering function) of the channel [1], [2]. We normalize the channel power seen by the system to unity, without loss of generality:

$$\begin{aligned} \sigma^2_H &= \frac{1}{TW}\int_0^T\int_{-W/2}^{W/2} E[|H(t,f)|^2]dtdf \\ &= \sum_{\ell,m}\sigma^2_{\ell,m} = \sum_{n=1}^{N_p} E[|\beta_n|^2] = 1. \end{aligned} \tag{11}$$

The number of delay-Doppler virtual channel coefficients represent the statistically independent *degrees of freedom* (DoF) in the channel - they are induced by a given physical channel model and the signaling scheme used. The number of DoF also represents the level of delay-Doppler diversity [13] afforded by the channel to combat fading and thus critically impacts the detection performance. In order to quantify the DoF, we define two key quantities:

$$D = L(2M-1) \approx TW\tau_{max}\nu_{max} \tag{12}$$

$$D_{eff} = |\{(\ell,m) : |S_{\tau,\ell}\cap S_{\nu,m}| \geq 1\}| \leq D \tag{13}$$

where D represents the *maximum* DoF – the maximum number of delay-Doppler resolution bins within the channel spreads (see Fig. 2) – and D_{eff} represents the *effective* number of DoF – the number of delay-Doppler bins that contain physical paths (red bins in Fig. 2).

Using the sampled virtual channel representation, we can make three observations. First, $D_{eff} \leq D$, where D increases linearly with the time-bandwidth product $N = TW$ (dimension of signal space). Second, for a physical model with a *finite* number of paths N_p, virtual path partitioning implies that $D_{eff} \leq N_p$ (see (7)). Thus, we conclude

$$D_{eff} \leq \min(N_p, D) = \min(N_p, TW\tau_{max}\nu_{max}). \tag{14}$$

Thirdly, if paths are distributed uniformly in delay and Doppler, we can approximate the expected value of D_{eff} from (10) by multiplying the probability that an individual bin is populated by D:

$$E[D_{eff}] \approx D\left(1-\left(\frac{D-1}{D}\right)^{N_p}\right). \tag{15}$$

Virtually all existing statistical channel models are implicitly based on the assumption of *rich multipath*, consisting of infinitely many diffuse scattering paths, influenced by the seminal WSSUS model for randomly linear time-varying channels introduced by Bello [2]. Under this assumption of rich scattering, all delay-Doppler bins will be populated with paths (see Fig. 2), regardless of how large TW is, resulting in $D_{eff} = D = TW\tau_{max}\nu_{max}$. Thus, in rich scattering, the channel exhibits the maximum number of DoF which scale linearly with TW.

Physical arguments as well as recent experimental results indicate that physical channels encountered in practice violate the assumption of rich scattering, especially at large bandwidths; see, for example, [3], [4] and references therein. Such physical environments will exhibit a *sparse* sampled channel representation, as illustrated in Fig. 2, in which $D_{eff} < D$. As the delay and/or Doppler resolution is increased, there will be some bins which are not populated by any paths and thus the corresponding $H_v(\ell,m)$ will contribute negligible power. We refer to such channels as *sparse* [3], [4].

A key observation, as illustrated in Fig. 3 (and also in Fig. 1), is that such physical channels will appear rich ($D_{eff} = D$) at low signaling duration and bandwidth, i.e. $N_p \gg TW\tau_{max}\nu_{max}$. As the bandwidth and/or signaling duration are increased, they will exhibit a progressively sparser structure (as $D = TW\tau_{max}\nu_{max}$ gets progressively large compared to N_p). D_{eff} will exhibit linear scaling with TW at low time-bandwidth products, followed by a sub-linear scaling at larger time-bandwidth products, followed by eventual saturation of D_{eff} to N_p (see (14)). We will revisit this observation in Sec. IV.

[3]This case can arise in ultrawideband channels leading to specular rather than Gaussian channel statistics.

III. Detector Structures

In this section, we develop the detection framework. We consider two types of non-coherent detectors that require minimal *a priori* knowledge about the channel: i) the energy detector (ED), which requires knowledge of only the channel spreads, and ii) the optimal non-coherent detector (ONCD) that requires knowledge of complete channel statistics. In both cases, we assume that the transmitted signal is of duration T and bandwidth W. Moreover, noisy estimates of the virtual channel coefficients $\{H_v(\ell,m)\}$ are available at the detector, such as in the delay-Doppler RAKE receiver for spread-spectrum systems [13]. In both cases, the detector decides between one of two hypotheses based on its D-dimensional received signal vector $\mathbf{r}$:

$$\begin{aligned} H_0 &: \mathbf{r} = \mathbf{w} && \sim \mathcal{CN}(\mathbf{0}, \sigma^2\mathbf{I}) \\ H_1 &: \mathbf{r} = \sqrt{\mathcal{E}}\mathbf{h} + \mathbf{w} && \sim \mathcal{CN}(\mathbf{0}, \mathcal{E}\mathbf{\Sigma_h} + \sigma^2\mathbf{I}) \end{aligned} \quad (16)$$

where $\mathbf{w}$ denotes the noise vector with variance σ^2, $\mathcal{E}$ denotes transmitted signal energy, and

$$\mathbf{h} = \mathrm{vec}(\mathbf{H_v}) \quad (17)$$

denotes the D-dimensional vector of virtual channel coefficients $\{H_v(\ell,m)\}$. As discussed in Sec. II, we assume the elements of $\mathbf{h}$ are independent:

$$\mathbf{\Sigma_h} = E[\mathbf{h}\mathbf{h}^H] = \mathrm{diag}(\sigma_1^2, ..., \sigma_{\mathrm{D}}^2) \quad (18)$$

where σ_d^2 is the vectorized version of $\sigma_{\ell,m}^2$, defined in 10.

The test statistic, Z, is a quadratic function of $\mathbf{r}$ for both detectors. The decision is based on a test threshold γ: if $Z > \gamma$, the detector decides H_1, otherwise the detector decides H_0. We assess the performance of the detectors based on the error probabilities: the probability of false alarm, P_{FA}, and the probability of missed detection, P_{MD}:

$$P_{FA} = P(Z > \gamma | H_0) \qquad P_{MD} = P(Z < \gamma | H_1). \quad (19)$$

Our main focus is on minimizing P_{MD} for a given fixed P_{FA}, which determines the desired threshold γ.

A. Energy Detector

The energy detector, requiring only knowledge of the delay and Doppler spread, $\{\tau_{max}, \nu_{max}\}$, is the simplest non-coherent detector. The the test statistic Z is given by

$$Z = \mathbf{r}^H\mathbf{r} = \sum_{d=1}^{D} |r_d|^2 \ . \quad (20)$$

Each term in the sum, under the two hypotheses, is given by

$$H_0 : |r_d|^2 = |w_d|^2 \qquad H_1 : |r_d|^2 = |\sqrt{\mathcal{E}}h_d + w_d|^2 \quad (21)$$

and, thus, under either hypotheses, each term is distributed as a chi-squared random variable with 2 degrees of freedom, equivalent to an exponential distribution:

$$|r_d|^2 \sim \chi_2^2 \equiv \exp(\lambda_d) \quad , \quad \lambda_d = \frac{1}{E[|r_d|^2]}. \quad (22)$$

The parameter λ_d evaluates to

$$H_0 : \lambda_d = \frac{1}{2\sigma^2} \qquad H_1 : \lambda_d = \frac{1}{2(\mathcal{E}\sigma_d^2 + \sigma^2)}. \quad (23)$$

The test statistic for the energy detector (20) is a sum of exponentially distributed random variables with parameters $\{\lambda_d\}$. Under H_0, $\lambda_1 = \lambda_2 = \cdots = \lambda_D \equiv \lambda$, and the test statistic has a chi-squared distribution with $2D$ degrees of freedom. Under H_1, if each channel coefficient has equal power, the test statistic is also distributed chi-squared with $2D$ degrees of freedom. If the channel coefficients have distinct powers, as in sparse channels, the $\{\lambda_d\}$ are distinct. In this case, the test statistic is distributed according to a *hypo-exponential* distribution (also denoted a *generalized Erlang distribution*) [15]. Hence,

$$\begin{aligned} H_0 &: Z \sim \mathrm{Hypo}\,(\lambda, ..., \lambda) \\ H_1 &: Z \sim \mathrm{Hypo}\,(\lambda_1, ..., \lambda_{\mathrm{D}})\,. \end{aligned} \quad (24)$$

Note that the chi-squared distribution is a special case of the *hypo-exponential* distribution. The *hypo-exponential distribution* has a cumulative density function which can be expressed in closed form as [15]

$$P(Z < z) = F(z) = 1 - \alpha^T e^{z\mathbf{\Theta}}\mathbf{1} \quad , \quad z \geq 0 \quad (25)$$

where

$$\mathbf{\Theta} = \begin{bmatrix} -\lambda_1 & \lambda_1 & 0 & \cdots & 0 \\ 0 & -\lambda_2 & \lambda_2 & 0 & \vdots \\ \vdots & & \ddots & \ddots & 0 \\ 0 & & & -\lambda_{D-1} & \lambda_{D-1} \\ 0 & \cdots & 0 & 0 & -\lambda_D \end{bmatrix}_{[D\times D]} \quad (26)$$

$$\mathbf{1} = [1 \ \ 1 \ \ ... \ \ 1]^T_{[D\times 1]} \qquad \alpha = [1 \ \ 0 \ \ ... \ \ 0]^T_{[D\times 1]} \quad (27)$$

and e is the exponential matrix operator.

B. Optimal Non-Coherent Detector

The optimal non-coherent detector (ONCD) assumes knowledge of the variance of the virtual channel coefficients and is based on the general form of the likelihood ratio given by

$$L(\mathbf{r}) = \frac{f(\mathbf{r}|H_1)}{f(\mathbf{r}|H_0)} = \frac{|\mathbf{\Sigma}_0|}{|\mathbf{\Sigma}_1|} e^{-\mathbf{r}^H(\mathbf{\Sigma}_1^{-1} - \mathbf{\Sigma}_0^{-1})\mathbf{r}}. \quad (28)$$

Under the distributions defined in (16), the log likelihood ratio is given by

$$\log L(\mathbf{r}) = \frac{\mathbf{r}^H\mathbf{r}}{\sigma^2} - \mathbf{r}^H(\mathcal{E}\mathbf{\Sigma_h} + \sigma^2\mathbf{I})^{-1}\mathbf{r} + \varsigma \quad (29)$$

$$\varsigma = |\sigma^2\mathbf{I}| - |\mathcal{E}\mathbf{\Sigma_h} + \sigma^2\mathbf{I}|$$

where the constant, ς, is absorbed into the threshold, γ.

Recall $\mathbf{\Sigma_h} = \mathrm{diag}(\mathbf{\Sigma_h}) = \mathrm{diag}(\sigma_1^2, ..., \sigma_{\mathrm{D}}^2)$, where σ_d^2 is the power in the d-th virtual channel coefficient. The log likelihood ratio can then be further simplified to

$$\log L(\mathbf{r}) = \mathbf{r}^H \left(\frac{\mathbf{I}}{\sigma^2} - \mathbf{A}^{-1} \right) \mathbf{r} - \varsigma \quad (30)$$

where

$$\mathbf{A} = \mathrm{diag}(\mathcal{E}\sigma_1^2 + \sigma^2, ..., \mathcal{E}\sigma_{\mathrm{D}}^2 + \sigma^2) \ . \tag{31}$$

The test statistic for the ONCD is given by

$$Z = \mathbf{r}^H \left(\frac{\mathbf{I}}{\sigma^2} - \mathbf{A}^{-1} \right) \mathbf{r} = \sum_{d=1}^{D} |r_d|^2 \left(\frac{1}{\sigma^2} - \frac{1}{\mathcal{E}\sigma_d^2 + \sigma^2} \right) \ . \tag{32}$$

As in the energy detector, under either hypothesis, each term of the sum will follow an exponential distribution:

$$|r_d|^2 \left(\frac{1}{\sigma^2} - \frac{1}{\mathcal{E}\sigma_d^2 + \sigma^2} \right) \sim \chi_2^2 \equiv \exp(\lambda_d) \tag{33}$$

$$\lambda_d = \frac{1}{E[|r_d|^2 (\frac{1}{\sigma^2} - \frac{1}{\mathcal{E}\sigma_d^2 + \sigma^2})]} \ . \tag{34}$$

We define the *per channel* signal to noise ratio (SNR) as

$$\mathrm{SNR}_d = \frac{\mathcal{E}\sigma_d^2}{\sigma^2} \ . \tag{35}$$

The parameter λ_d is given by

$$\begin{aligned} H_0 \quad &: \quad \lambda_d = \frac{\mathcal{E}\sigma_d^2 + \sigma^2}{2\mathcal{E}\sigma_d^2} = \frac{1}{2} + \frac{1}{2\mathrm{SNR}_d} \\ H_1 \quad &: \quad \lambda_d = \frac{\sigma^2}{2\mathcal{E}\sigma_d^2} = \frac{1}{2\mathrm{SNR}_d}. \end{aligned} \tag{36}$$

The test statistic under either hypothesis is a sum of exponential random variables. As before, Z has a *hypo-exponential* distribution.

$$\begin{aligned} H_0 \quad &: \quad Z \sim \mathrm{Hypo}\left(\frac{1}{2} + \frac{1}{2\mathrm{SNR}_1}, ..., \frac{1}{2} + \frac{1}{2\mathrm{SNR}_D} \right) \\ H_1 \quad &: \quad Z \sim \mathrm{Hypo}\left(\frac{1}{2\mathrm{SNR}_1}, ..., \frac{1}{2\mathrm{SNR}_D} \right) \end{aligned} \tag{37}$$

IV. Discussion and Results

In this section, we present numerical results for comparing the performance of the two non-coherent detectors in sparse multipath channels: the energy detector (ED) that requires knowledge of only channel spreads (τ_{max}, ν_{max}) and the optimal non-coherent detector (ONCD) that requires full statistical channel knowledge. For both detectors, the test statistic is distributed according to a *hypo-exponential* distribution, each with different parameters $\{\lambda_d\}$ which depend on the variance of the *virtual channel coefficients*, $\{\sigma_d^2\}$, and the operating SNR. The total degrees of freedom of the channel, D, define the number of parameters of the distribution.

We first present results for frequency-selective channels in which D is a function of only bandwidth. Frequency-selective channels can be viewed as a specific case of the more general doubly-selective channel. We use the development in Sec. III to compare the detection performance for the two detectors as a function of the signal bandwidth, W, and SNR for three representative multipath environments: rich ($N_p = 500$), medium rich ($N_p = 50$), and sparse ($N_p = 10$). In all cases, $\tau_{max} = 10\mu$s ($\nu_{max} \approx 0$Hz), the path gains have equal power, and the path delays are uniformly distributed within $[0, \tau_{max}]$.

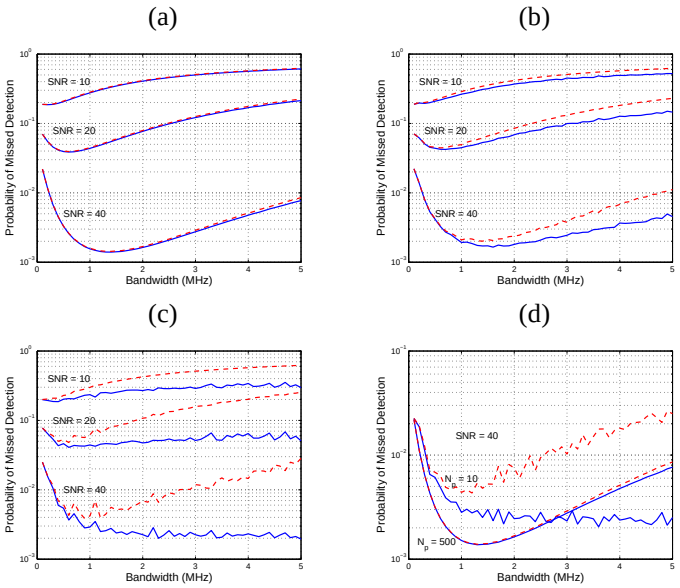

Fig. 4. **(a) - (c)** Probability of missed detection as a function of bandwidth for three frequency selective multipath environments ($\tau_{max} = 10\mu$s): **(a)** $N_p = 500$, **(b)** $N_p = 50$, and **(c)** $N_p = 10$. At the highest bandwidth, $D = W\tau_{max} = 50$. $P_{FA} = 0.05$ in all cases. The dashed lines show performance of the ED, while the solid lines show performance of the ONCD. For comparison, **(d)** shows P_{MD} for rich and sparse channels on the same plot.

For each scattering environment, the variance of the D channel coefficients, $\{\sigma_d^2\}$, are calculated using the exact expression found in (10). They are then normalized as

$$\sum_{d=1}^{D} \sigma_d^2 = 1 \tag{38}$$

and are related to the total average SNR as

$$\mathrm{SNR} = \frac{\mathcal{E}}{\sigma^2} = \sum_{d=1}^{D} \frac{\mathcal{E}\sigma_d^2}{\sigma^2} = \sum_{d=1}^{D} \mathrm{SNR_d}. \tag{39}$$

For a given P_{FA}, the cumulative density function of the test statistic, under H_0, can be inverted numerically to find the corresponding threshold γ. The detector performance is assessed via P_{MD} for the corresponding threshold. P_{MD} is calculated using the closed-form expression for the *hypo-exponential* distribution in (25), under H_1.

A. Frequency-Selective Channel

Fig. 4(a) shows results at three SNRs for the rich multipath environment consisting of $N_p = 500$ paths. Both detectors behave similarly since, even at maximum bandwidth of 5MHz, $D_{eff} = D = 50 \ll N_p$ and the channel coefficients have nearly identical power. Furthermore, the results indicate an optimal bandwidth, W_{opt}, at which P_{MD} is minimum. In rich multipath, it is empirically noted in [1] that the optimal[4] level of diversity is $D_{opt} \approx \mathrm{SNR}/3$ which corresponds to $W_{opt} \approx \frac{\mathrm{SNR}}{3\tau_{max}}$. This agrees with our results: a bandwidth of

[4]Optimal in the sense that the probability of bit error for binary signaling is minimized; nonetheless, the empirical results applies to the detection problem.

1.3 MHz corresponds to $D = 13$ at the SNR of 40 (linear units). We borrow this empirical result for the remainder of our discussions.

Fig. 4(b) shows corresponding results for the medium rich environment. The performance of the ED and ONCD coincide for lower values of W as $D_{eff} \approx D$, since $N_p > D$ (see (14)). However, as W increases, the performance of the ED worsens compared to the ONCD since some of the virtual channel coefficients exhibit near-zero power. As a result, $D_{eff} < D$. The ED picks up noise in those coordinates, whereas the ONCD nulls them out due to complete statistical knowledge.

Fig. 4(c) shows the performance of both detectors in the sparse regime. At approximately 500 kHz, corresponding to $D = 5$, the ONCD begins to substantially outperform the ED. As bandwidth increases further into the sparse regime, so that $D > N_p$, the performance of the ONCD remains nearly constant as D_{eff} is bounded by N_p.

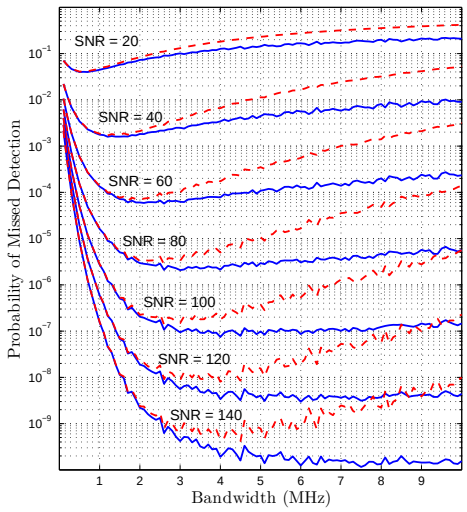

Fig. 5. P_{MD} for SNRs from 20 to 140 (linear units). $\tau_{max} = 10\mu$s. $N_p = 50$. $P_{FA} = 0.05$. The dashed lines show the performance of the ED, while the solid line shows performance of the OCND. For the OCND, beyond $\approx$ 5MHz, increasing bandwidth has little effect on performance, as the channel appears sparse, and D_{eff} is bounded by N_p. For high SNR, $D_{opt} \approx \text{SNR}/3 = 50 = N_p$ and optimal performance is maintained as bandwidth is increased.

Figure 5 expands on Fig. 4(b) for a greater range of SNRs and for larger bandwidths to highlight the trends in P_{MD}. The trends in Figure 5 are best understood by referencing Fig. 3 which was also generated for $N_p = 50$. As the bandwidth is increased, the channel characteristics transition from "rich" to "medium rich/sparse" to "sparse". At low bandwidths, less than 1MHz, the multipath channel still appears rich. In this regime, $N_p \gg D$ and, thus, $D_{eff} = D \approx W\tau_{max}$. As bandwidth increases, we enter the medium rich regime and, as evident in Fig. 3, D_{eff} exhibits sub-linear growth with bandwidth W (TW in the doubly selective case). Finally, as W is increased further, we enter the sparse regime in which D_{eff} saturates to N_p (see (14)) and performance remains nearly constant.

B. Doubly-Selective Channel

Doubly-selective channels, a generalization of the frequency-selective case, exhibit parallel results. Fig. 6 displays the performance of the ONCD as a function of both signaling duration and bandwidth. The left figure shows P_{MD} for a rich a channel in which $D_{eff} \approx D < N_p$. The right figure shows P_{MD} for a sparse channel in which D_{eff} saturates to N_p as the signaling dimension is increased. Performance remains nearly constant beyond saturation. The surface color indicates the signaling dimension (time-bandwidth product, TW). For channels with uniformly distributed delay and Doppler, the performance of the detector is a function of the product of signaling duration T and bandwidth W; statistically, performance remains constant for a fixed TW, regardless of changes in the ratio T/W.

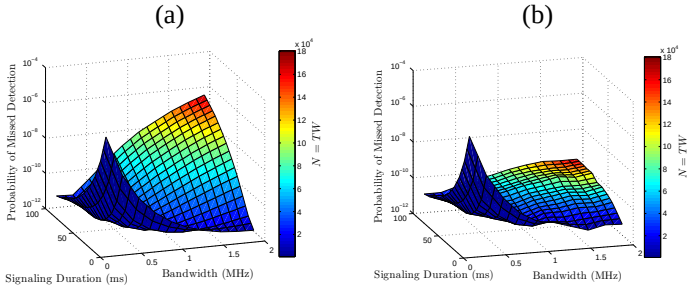

Fig. 6. Doubly-selective channels. SNR 150 (linear units). $\tau_{max} = 10\mu$s, $\nu_{max} = 200$Hz. (a) $N_p = 500$, (b) $N_p = 50$. The color of the surface indicates the time-bandwidth product, $N = TW$.

C. Discussion

For the ONCD, the optimal signaling dimension (time-bandwidth product) can be predicted by combining the expected value of D_{eff} (equation (15)) with the empirical results from [1], $D_{opt} = \text{SNR}/3$. For any multipath channel, rich or sparse, we estimate the optimal total degrees of freedom, D_{opt}, as the solution to:

$$E[D_{eff}] = D_{opt}\left(1 - \left(\frac{D_{opt}-1}{D_{opt}}\right)^{N_p}\right) = \frac{\text{SNR}}{3} \qquad (40)$$

over the range

$$D_{opt} \in [0, \infty) \leftrightarrow \text{SNR}/3 \in [0, \text{N}_\text{p}].$$

We can then calculate the optimal transmit dimension using $D = TW\tau_{max}\nu_{max}$.

Fig. 7 graphs equation (40). The left axis shows the expected optimal bandwidth for a frequency selective channel, such as that shown in Fig. 5. The optimal bandwidth predicted by (40) agrees with Fig. 5 - for instance, at an SNR of 100, (40) predicts an optimal bandwidth of 5.5MHz - Fig. 5 shows a minimum P_{MD} at or near this bandwidth.

The range of equation (40) suggests we characterize physical multipath channels into three regimes:

$$N_p < \frac{\text{SNR}}{3} \qquad N_p \approx \frac{\text{SNR}}{3} \qquad N_p > \frac{\text{SNR}}{3}$$

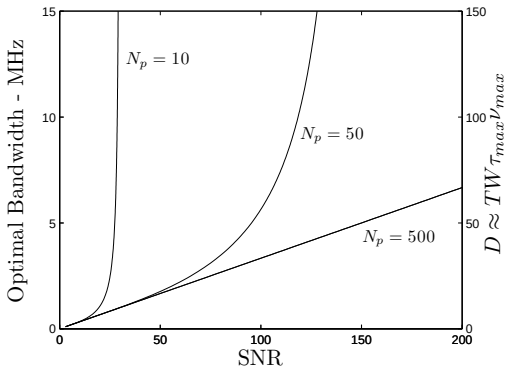

Fig. 7. Optimal degrees of freedom, D, as a function of SNR for three multipath environments: $N_p = 10$, $N_p = 50$, $N_p = 500$. The left axis shows the corresponding bandwidth for a frequency selective channel with $\tau_{max} = 10\mu$s.

When $N_p < \frac{\mathrm{SNR}}{3}$, equation (40) has no solution; the multipath diversity afforded by the channel is insufficient to achieve the optimal degrees of freedom for that SNR. Regardless of increase in signaling dimension, the effective degrees of freedom of the channel are bounded by N_p, which is less than the optimal level, and performance remains worse than that of the optimal achieved in a corresponding rich channel. Fig. 3 aids in visualization of this scenario - if $\mathrm{SNR} > 150$, D_{eff}, bounded by N_p, never reaches D_{opt}.

In the next regime, $N_p \approx \frac{\mathrm{SNR}}{3}$, and the multipath diversity of the channel is sufficient to achieve the optimal performance of the corresponding rich channel. As the signaling dimension ($N = TW$) is increased, D_{eff} increases at a sublinear rate, but eventually saturates to N_p. Beyond the optimal signaling dimension, performance does not decrease as it would in the corresponding rich channel; again, the effective degrees of freedom, bounded by N_p remain at a near optimal level regardless of increase in signaling dimension. In Fig. 3, the horizontal line with $\mathrm{SNR} = 150$ exhibits this regime. The solid line, D_{eff}, approaches D_{opt} asymptotically.

When $N_p > \frac{\mathrm{SNR}}{3}$, an optimal signaling dimension exists. If the signaling dimension is increased beyond this optimum, performance deteriorates at a rate less than or equal to the rate of the corresponding rich multipath channel. The horizontal line in Fig. 3 with $\mathrm{SNR} = 60$ exhibits this scenario. The optimal D_{eff} is reached at nearly the same signal dimension as the corresponding rich channel.

V. Conclusion

We have developed and characterized the performance of two non-coherent detectors in sparse multipath channels. The optimal non-coherent detector, which exploits statistical channel knowledge, weights the received signal vector based on the variance of the virtual channel coefficients. The energy detector simply combines the energy in each virtual channel coefficient. Both detectors result in a test statistic with a *hypo-exponential* distribution.

We explored the notion of *effective* degrees of freedom for a sparse multipath channel; in sparse channels, the performance of the two detectors depends critically on the effective degrees of freedom afforded by the channel. In rich multipath, the performance of the energy detector is nearly identical to that of the optimal non-coherent detector. As the sparsity of multipath increases, the performance of the energy detector deteriorates as compared to the optimal non-coherent detector.

In rich multipath, as noted in [1], optimal signal detection occurs when the total degrees of freedom are $D \approx \mathrm{SNR}/3$. Utilizing the notion of effective degrees of freedom, we presented a unifying expression that predicts the optimal degrees of freedom of a channel in both rich and sparse multipath. The optimal degrees of freedom correspond to a signaling dimension (time-bandwidth product) which maximizes the probability of detecting a signal.

Looking forward, the authors would like to further explore the impact of the fundamental relationship between SNR and effective degrees of freedom on detection performance. Additionally, the authors plan to expand the work to encompass multipath environments with non-uniformly distributed delay and Doppler and relax the requirement of normally-distributed virtual channel coefficients.

References

[1] J. G. Proakis, *Digitial Communications*, 4th ed. New York: McGraw Hill, 2002.

[2] P. A. Bello, "Characterization of randomly time-variant linear channels," *IEEE Trans. Commun. Syst.*, vol. CS-11, pp. 360–393, Nov. 1963.

[3] A. Sayeed, "Sparse multipath channels: Modeling and implications," *Adaptive Sensor Array Processing Workshop*, 2006.

[4] W. Bajwa, A. Sayeed, and R. Nowak, "Sparse multipath channels: Modeling and estimation," *IEEE Digital Signal Processing and Signal Processing Education Workshop*, 2009.

[5] F. Lee and P. Mclane, "Parallel-trellis turbo equalizers for sparse-coded transmission over SISO and MIMO sparse multipath channels," *IEEE Transactions on Wireless Communications*, vol. 5, pp. 3568–3578, Dec. 2006.

[6] L. Hanlen, R. Timo, and R. Perera, "On dimensionality for sparse multipath," *Proceedings. 7th Australian Communications Theory Workshop, 2006.*, pp. 125–129, Feb. 2006.

[7] S. Chowdhury, M. Zoltowski, and J. Goldstein, "Structured MMSE equalization for synchronous CDMA with sparse multipath channels," *Proceedings. (ICASSP '01). 2001 IEEE International Conference on Acoustics, Speech, and Signal Processing, 2001.*, vol. 4, pp. 2113–2116, May 2001.

[8] A. F. Molisch, "Ultrawideband Propagation Channels - Theory, Measurement and Modeling," *IEEE Trans. Veh. Tech.*, Sept. 2005.

[9] "Special issue on dynamic spectrum access," *IEEE Journal on Selected Topics in Signal Processing*, Feb. 2008.

[10] "Special issue on cognitive radio," *Proceedings of the IEEE*, Apr. 2009.

[11] I. M. A. Goldsmith, S. A. Jafar and S. Srinivasa, "Breaking spectrum gridlock with cognitive radios: An information theoretic perspective," in *Proceedings of the IEEE*, 2009.

[12] R. Tandra and A. Sahai, "SNR walls for signal detection," in *IEEE Journal on Selected Topics in Signal Processing*, Feb. 2008, pp. 4–17.

[13] A. M. Sayeed and B. Aazhang, "Joint multipath-Doppler diversity in mobile wireless communications," *IEEE Trans. Commun.*, vol. 47, no. 1, pp. 123–132, Jan. 1999.

[14] A. M. Sayeed and V. Veeravalli, "The essential degrees of freedom in space-time fading channels," in *Proc. 13th IEEE International Symposium on Personal, Indoor and Mobile Radio Communications (PIMRC'02)*, Lisbon, Portugal, Sep. 2002, pp. 1512–1516.

[15] M. F. Neuts, *Matrix-Geometric Solutions in Stochastic Models: An Algorithmic Approach*, revised edition ed. Dover Publications, 1995.